

## Aerodynamic Shape Optimization of Vehicles Using CFD Simulation

Ahmed Zawad Ul Hoque\*, Mohammad Ariful Islam, Md. Ahatashamul Haque Khan Shuvo

Department of Mechanical Engineering, Khulna University of Engineering & Technology, Khulna-920, BANGLADESH

### ABSTRACT

With the significant improvement of battery technology and manufacturing methods in the last two decades, the automotive industries worldwide are shifting towards more environment-friendly electric and hybrid-electric vehicles rather than fuel based combustion engine vehicles. Aerodynamic shape optimization of vehicles still holds a large potential for cuts in emissions. Drag and lift characteristics of a vehicle play a key role in vehicle aerodynamics and therefore, an active area of research for automobile manufacturers. This paper approaches computational fluid dynamics (CFD) simulation for some of the major design parameters that affect the vehicle aerodynamics. Geometrical bodies of “Ahmed body” and 3 common vehicle types i.e. Sedan, Compact Utility Vehicle (CUV), Truck had been created. Then airflow around the vehicles was simulated to calculate lift and drag coefficients. Also, experimental drag coefficient value for “Ahmed Body” had been validated by CFD simulation before performing design modifications and further simulations. Finally, obtained values of drag and lift coefficients were compared with the benchmark value.

Keywords: Aerodynamics, Shape Optimization, Vehicle, Drag, Lift, CFD, Simulation

### 1. Introduction

Since the invention of automobile, there had been tremendous developments in the automotive industries. And yet, climate change due to the emissions of automobiles remains one of the key concerns of the 21<sup>st</sup> century. As drastic changes occurred in the climate due to the increased emissions of CO<sub>2</sub> in the recent years, an act passed by the European Union in 2009 urged to reduce the emissions of greenhouse gases by 20% within 2020 compared to the levels of 1990 [1]. This act has pushed the automotive industries to further development of economical vehicles which are both environment friendly and fast. At highway speeds, overcoming aerodynamic drag is responsible for more than 50 percent of fuel consumption [2]. Hence, improving the aerodynamic shape will result in significant reduction in drag force and improved fuel economy & emissions.

Vehicle aerodynamics is a science in continuous development and research. In contrast to other technical disciplines which are mainly governed by well-established theoretical and experimental methods of fluid mechanics, there are no consistent design procedures available for road vehicles yet. The flow fields around a car characterized by separation are so complex that the vehicle aerodynamicist must make references to a large amount of data from earlier works and his triumph resides on his ability to transfer and combine results originating from many different earlier developments into his own problem for a consistent solution.

For the proper understanding of vehicle aerodynamics, first it's needed to identify the common design parameters. Then the flow around the vehicle is

considered and from it the drag and lift coefficient of the vehicle comes into play. To improve aerodynamic characteristics, the drag coefficient of the vehicle must be reduced to such a limit that the other aerodynamic properties of the vehicle also remain at a considerable point. Aerodynamic drag (D) increases with the square of vehicle speed (V) as shown in Eq. (1).

$$D \sim V^2 \quad (1)$$

The complete expression of Eq. (1) is

$$D = C_D A \frac{\rho}{2} V^2 \quad (2)$$

Where, A is projected frontal area and  $\rho$  is the density of the surrounding air. The drag D of a vehicle is therefore determined by its frontal area A, and by its shape, the aerodynamic quality of which is described by the drag coefficient  $C_D$ . Generally the vehicle size, and hence frontal area, is determined by the design requirements, and efforts to reduce drag are concentrated on reducing the drag coefficient [2].

The objectives of this paper are to identify common design parameters that affect the vehicle aerodynamics, to simulate the air flow around the vehicle for obtaining an accurate value of its drag and lift coefficient and to make modifications to the vehicle geometry which could improve its lift and drag characteristics.

### 2. Optimization Method

There are a number of different methods for optimizing the aerodynamic shape of a vehicle but they all share some common aspects. The schematics of a general

\* Corresponding author. Tel.: +88-01919303838, +88-01748714374

Email addresses: hoque.me.kuet@gmail.com, ariful@me.kuet.ac.bd, mahsk1320@yahoo.com

method which had been followed in this paper for optimizing the aerodynamic shape of the vehicles can be seen in Fig.1.

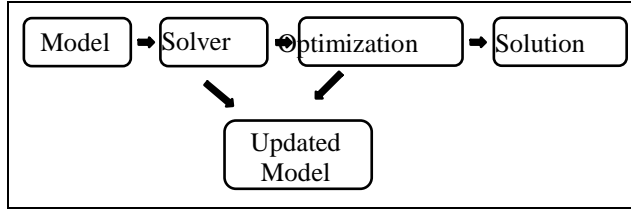


**Fig.1** A schematic diagram of the general method for the aerodynamic shape optimization

CFD simulation is performed on an initial model. The result is analyzed by using some optimization algorithm. Some design parameters of the model are updated and a new CFD simulation is performed on the updated model. This iterative process continues until some stop condition is reached. Due to longer computational periods, only simplified models or coarse meshes are used in this method. The large computational cost associated with this method limits the real-world applications for the automotive industry at present day [3].

Simulation of vehicle shape optimization was performed on ANSYS Fluent which uses a Finite Volume Method (FVM) to solve the governing equations by discretization and integration over the finite volume [4]. Standard k-ε turbulent model was used. It is a semi-empirical, two-equation model, including two transport equations that represent the turbulent properties of the flow. The first transported variable is turbulent kinetic energy, k. The second transported variable in this case is the turbulent dissipation, ε. It is the variable that determines the scale of the turbulence, whereas the first variable, k, determines the energy in the turbulence [5].

#### 4. Governing Equations

The continuity equation in Eq. (4) and momentum equations (also known as Navies - Stokes equations) in Eq. (5) – Eq. (7) with a turbulence model were used to solve the airflow

$$\frac{\partial u}{\partial x} + \frac{\partial v}{\partial y} + \frac{\partial w}{\partial z} = 0 \quad (4)$$

$$u \frac{\partial u}{\partial x} + v \frac{\partial v}{\partial y} + w \frac{\partial w}{\partial z} = -\frac{1}{\rho} \frac{\partial p}{\partial x} + \frac{1}{\rho} \left( \frac{\partial \tau_{xy}}{\partial y} + \frac{\partial \tau_{xz}}{\partial x} \right) + B_x \quad (5)$$

$$u \frac{\partial u}{\partial x} + v \frac{\partial v}{\partial y} + w \frac{\partial w}{\partial z} = -\frac{1}{\rho} \frac{\partial p}{\partial y} + \frac{1}{\rho} \left( \frac{\partial \tau_{xy}}{\partial y} + \frac{\partial \tau_{yz}}{\partial x} \right) + B_y \quad (6)$$

$$u \frac{\partial u}{\partial x} + v \frac{\partial v}{\partial y} + w \frac{\partial w}{\partial z} = -\frac{1}{\rho} \frac{\partial p}{\partial z} + \frac{1}{\rho} \left( \frac{\partial \tau_{xz}}{\partial y} + \frac{\partial \tau_{yz}}{\partial x} \right) + B_z \quad (7)$$

Where  $u$  is  $x$ -component of velocity vector,  $v$  is  $y$ -component of velocity vector and  $w$  is  $z$ -component of velocity vector.  $\rho$  is density of air,  $p$  is static pressure,  $\tau$  is shear stress and  $B_x, B_y, B_z$  are body forces [6].

#### 4.1 Transport equations for standard k - εturbulent model:

For turbulent kinetic energy k:

$$\frac{\partial}{\partial t}(\rho k) + \frac{\partial}{\partial x_i}(\rho k u_i) = \frac{\partial p}{\partial x_j} \left[ \left( \mu \frac{\mu_t}{\sigma_k} \right) \frac{\partial k}{\partial x_j} \right] + G_k + G_b - \rho \epsilon - Y_M - S_k$$

For dissipation ε:

$$\frac{\partial}{\partial t}(\rho \epsilon) + \frac{\partial}{\partial x_i}(\rho \epsilon u_i) = \frac{\partial p}{\partial x_j} \left[ \left( \mu \frac{\mu_t}{\sigma_\epsilon} \right) \frac{\partial \epsilon}{\partial x_j} \right] + C_{1e} \frac{\epsilon}{k} (G_k + C_{3e} G_b) - C_{2e} \rho \frac{\epsilon^2}{k} + S_\epsilon$$

In these equations,  $G_k$  represents the generation of turbulence kinetic energy due to the mean velocity gradients.  $G_b$  is the generation of turbulence kinetic energy due to buoyancy.  $Y_M$  represents the contribution of the fluctuating dilatation in compressible turbulence to the overall dissipation rate.  $C_{1e}, C_{2e}$  and  $C_{3e}$  are constants.  $\sigma_k$  and  $\sigma_\epsilon$  are the turbulent Prandtl numbers for k and ε, respectively.  $S_k$  and  $S_\epsilon$  are user-defined source terms [6].

The model constants  $C_{1e}, C_{2e}, C_{3e}, \sigma_k$  and  $\sigma_\epsilon$  have the following default values:  $C_{1e} = 1.44, C_{2e} = 1.92, C_{3e} = 0.09, \sigma_k = 1.0, \sigma_\epsilon = 1.3$ . These default values have been determined from experiments with air and water for fundamental turbulent shear flows including homogeneous shear flows and decaying isotropic grid turbulence [6]. They have been found to work fairly well for a wide range of wall- bounded and free shear flows [6].

#### 5. Numerical Modeling

For the analysis, the geometry of vehicle was modeled using SolidWorks 2017, where the boundary of the vehicle was formed by tracing curves from the unofficial blueprints of the model. Then the model was converted to solid part and simplified before importing to ANSYS Design Modeler. In this study, 3 types of vehicle were analyzed where the experimental and computational results of “Ahmed Body” was used to validate the other results. The “Ahmed Body” was first created by S.R. Ahmed in 1984 [7]. In vehicle’s industry, Ahmed Car Body is the standard model that can be used as validating case, in industry and CFD simulation [8]. The other vehicle types were Sedan, CUV, Cargo Truck and their respective bodies after geometrical modifications.

A 12500 mm× 3000 mm× 3000 mm fluid flow field enclosure had been created where the enclosure acted as air. The front of the body is placed at a distance of 2 car lengths (2L) from the flow inlet and at a distance of 6 car

lengths (6L) from the flow outlet. A symmetry plane is introduced to model half of the model with an aim to reduce the computational time.

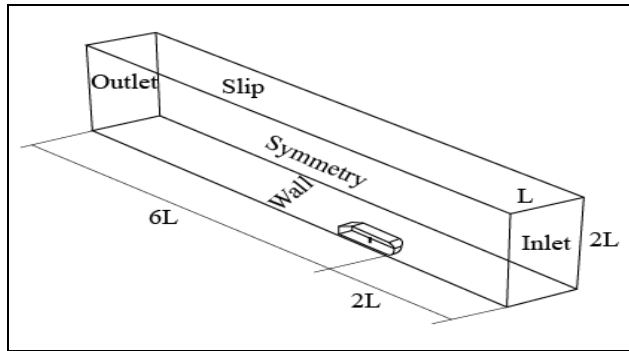


**Fig.2** Computational domain for the simulation

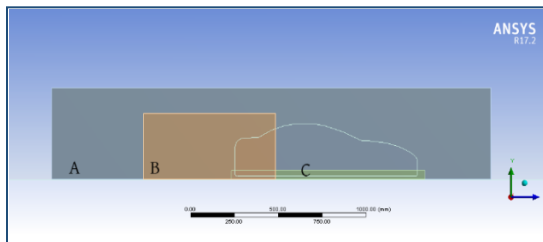


**Fig.3** Fine mesh boxes inside the computational domain for Sedan type vehicle analysis (sample image)

**Table 1** Cell sizes in each refinement box

Area	Cell Element Size (High Mesh)	Cell Element Size (Low Mesh)
Around Car (A)	10 mm	100 mm
Wake (B)	10 mm	100 mm
Under Car (C)	15 mm	150 mm

A finer mesh downstream of the model was used to capture the wake zone. The cell element size was varied from 10 mm to 150 mm at a growth rate of 1.2. While creating the mesh, 3 different sizing functions had been used to obtain accurate lift & drag characteristics. Three bodies (Box A, Box B and Box C) of refinements as shown in Fig.3 and Table 1 were added to properly capture the flow in the region closest to the vehicle and the flow in the wake. The total number of nodes and elements for corresponding high & low meshes are shown in Table 2.

For boundary conditions, the enclosure inlet plane was named “velocity-inlet”. Air coming through the inlet was given a velocity of 40 m/s. The road and the vehicle body were both made walls & corresponding enclosure surface was named symmetry plane having a “no slip” condition. The outlet was named a “pressure-outlet” with a constant

**Table 2** Total number of nodes and elements

Geometry	Nodes (High)	Elements (High)	Nodes (Low)	Elements (Low)
Ahmed body	386856	1813949	72379	237868
Sedan	763911	2983666	238229	737570
Modified Sedan	707603	2805471	207009	644505
CUV	584947	2545238	138981	478941
Modified CUV	569018	2456256	122331	413021
Truck	1210102	4896517	199281	608368
Modified Truck	1267364	5120525	272219	872608

pressure equal to the atmospheric pressure. The flow is solved with a steady-state pressure-based Navier-Stokes solver in Fluent. As the strengths and weaknesses of the standard k-ε model have become known, modifications have been introduced to improve its performance. Two of these variants are available in ANSYS FLUENT: the RNG k-ε model and the realizable k-ε model. The term “realizable” means that the model satisfies certain mathematical constraints on the Reynolds stresses, consistent with the physics of turbulent flows. Neither the standard k-ε model nor the RNG k-ε model is realizable [5]. A realizable k-ε turbulence model is used together with a second-order discretization scheme for pressure and momentum and a first-order discretization scheme for k and ε.

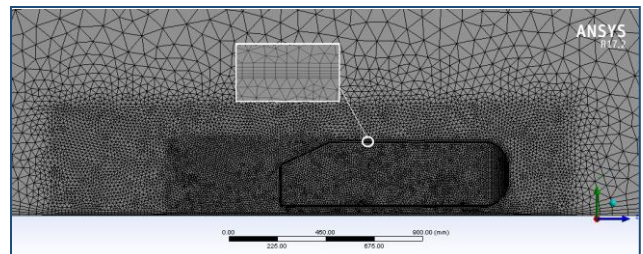


**Fig.4** Final Mesh of Ahmed body 25 degree slant with different sizing functions (sample image of mesh)

### 5.1 Model Optimization Study:

A total of six studied design parameters were roof drop, underbody hoist, diffuser hoist, boat tailing, wing mirrors removal and addition of spoiler. The limits were chosen as the maximum changes that would still produce a realistic

**Table 3** Design parameter limits

Parameter	Baseline	Maximum
Roof Drop	0	100 mm
Underbody Hoist	0	107 mm
Diffuser Hoist	0	100 mm
Boat Tailing	0	50 mm

car. Some of these design parameters had been experimented and optimized by Anton Lundberg [3] and were applied in this analysis with a mission to produce a satisfactory drag reduction rate.

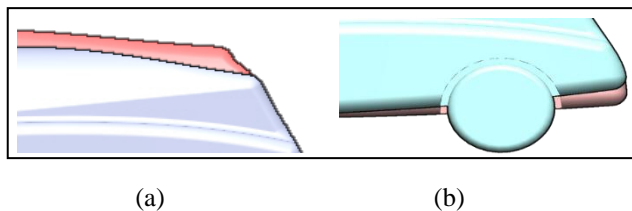


**Fig.5** (a) Comparison of baseline (colored red in background) and fully morphed (colored blue in foreground) roof. (b) Comparison of baseline (colored red in background) and fully morphed (colored blue in foreground) diffuser.

A roof drop was achieved by compressing a portion of the roof from the highest point to the rear end. The compression had a linear variation with full compression at the highest point of the roof. A comparison of the baseline and the maximum roof drop of 100 mm can be seen in Fig.5. The diffuser was changed by moving the rear edge upwards by a maximum distance of 100 mm.

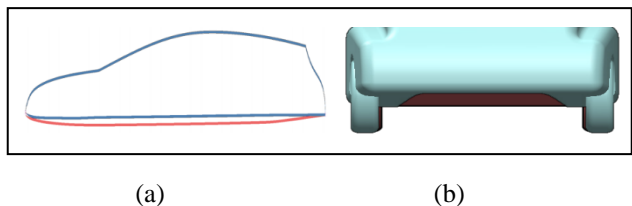


**Fig.6** (a) Comparison of baseline (colored in red) and fully morphed (colored in blue) underbody contours. (b) Comparison of baseline (colored red in background) and fully morphed (colored blue in foreground) underbody as seen from the front.

The baseline underbody has a curvature along the car. The underbody was hoisted to achieve the latter profile. The maximum underbody hoist was 107 mm, at which point the underbody was flat as shown in Fig.6

The rear end was slimmed by moving the rear side edge of the car inwards. This is known as boat tailing. A comparison of the baseline and the maximum boat tailing of 50 mm can be seen in Fig.7.

Wing mirrors also known as side view mirrors do impact vehicle aerodynamics and fuel economy. But as an alternative to conventional wing mirrors, the use of cameras could help in reducing aerodynamic drag by an average of 2-7% [2]. This method had been applied by many of the modern automakers like Tesla, Volkswagen, Volvo, especially, in their electric vehicles and gaining popularity day by day.

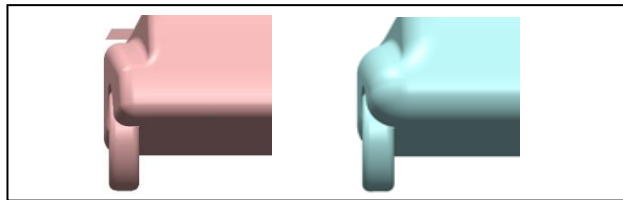


**Fig.7** Comparison of baseline and fully morphed rear. In the fully morphed case a boat tailing is applied, i.e. the rear is slimmed by moving the rear edge inwards. The maximum boat tailing is 50 mm.

Spoilers are not only used on sedan type race cars and road cars to provide downward force, but also to resist the natural tendency of these cars to become “light” in the rear because of the lift generated by the rear body shape. They act like barriers to air flow which results into a buildup of higher air pressure in front of the spoiler, therefore, helping to stabilize the lighter rear portion of car stick to the road.

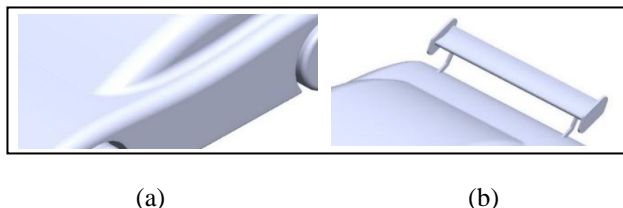


**Fig.8** (a) Wing Mirror removed in Modified Sedan (b) Spoiler added to Modified Sedan

## 6. Results & Discussion

The computational drag and lift co-efficient values of the “Ahmed Body” was found in close agreement with the experimental values as shown in Table 5 [10] and Fig. 9

**Table 4** Comparative  $C_D$  and  $C_L$  values of Ahmed Body

Ahmed Body ( $\alpha=25^\circ$ )	Experimental Value	Computational Value
$C_D$	0.299	0.286
$C_L$	0.345	0.381

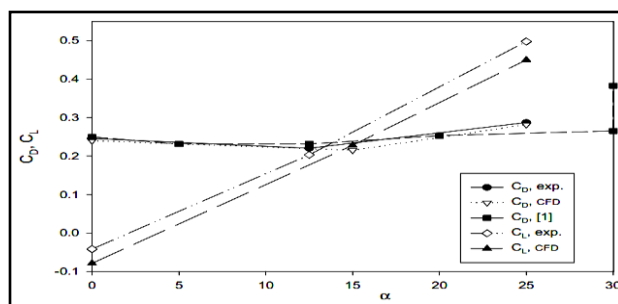


**Fig.9** Comparisons of  $C_D$  and  $C_L$  from present computational and experimental (exp) studies and the experimental data from ref. [7] (Fig. ref. [11])



Therefore, the computational data of the “Ahmed Body” is validated by the mentioned experimental data which had been used as a benchmark value throughout rest of the CFD simulations.

Fig.10 depicts a series of comparative illustration of velocity streamlines between the initial and the modified bodies of the subject vehicles. These figures demonstrate that the air velocity decreases as it approaches the frontal

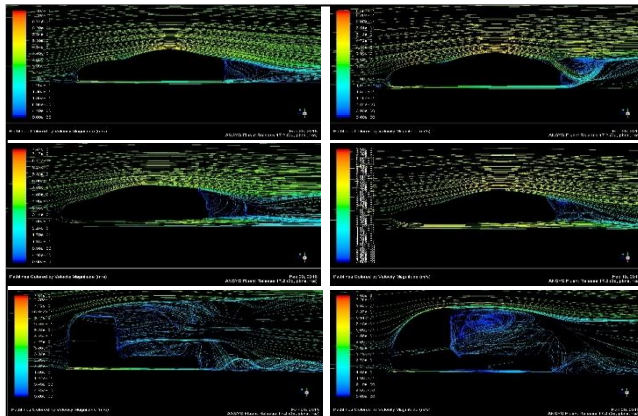


**Fig.10** Streamlines of Velocity Magnitude (m/s)

section of the vehicles and then increases away from the front. In modified bodies, the velocity magnitude decreases from a higher gradient, therefore, indicating that the air resistance is smaller.

**Table 5** Comparison of Velocity Magnitude (m/s) Gradients

Geometry	Initial Gradient Range (m/s)	Modified Gradient Range (m/s)
Sedan	0-7.49E+1	0-6.56E+1
CUV	0-7.47E+1	0-6.43E+1
Truck	0-7.91E+1	0-7.58E+1

Fig.11 illustrates the comparative static pressure contours of the subject bodies. It is evident from the images that there is a higher pressure concentration on the vehicle front, windshield and wing mirror in all cases. But this pressure concentration is dropped significantly when the wing mirrors of the vehicles had been removed and the frontal curve of the vehicles are less steeper after performing the geometrical modifications.

Particularly, the air slows down when it approaches the front of the car and results in that more air molecules are accumulated into a smaller space. Once the air stagnates in front of the car, it seeks a lower pressure area, such as the sides, top and the bottom of the car. As the air flows over the car hood, pressure is decreasing, but when it reaches the front windshield, it increases briefly [9]. As

the high pressure air glides over the windshield, it accelerates and causes a decrease of the pressure which results into a lift - force on the car roof as the air passes over it.

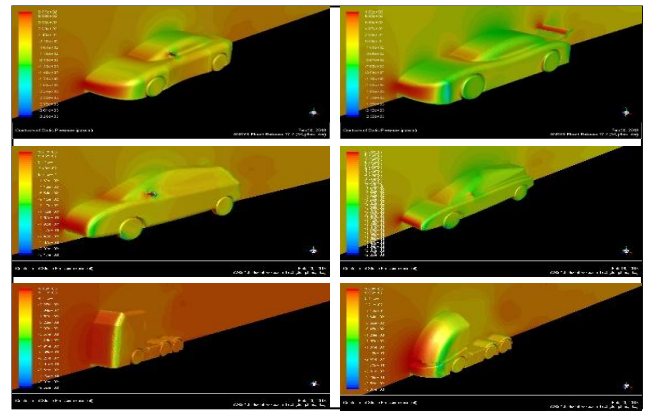


**Fig.11** Contours of Static Pressure (Pa)

Fig.12 shows the contours of Wall  $y^+$  for all cases. As the turbulence model wall laws have restrictions on the  $y^+$  value at the wall. So, for each turbulence model it should be determined in appropriate way. It had been observed from contours that the  $y^+$  values fall into the required range of  $30 < y^+ < 300$  for  $k-\epsilon$  turbulence model.

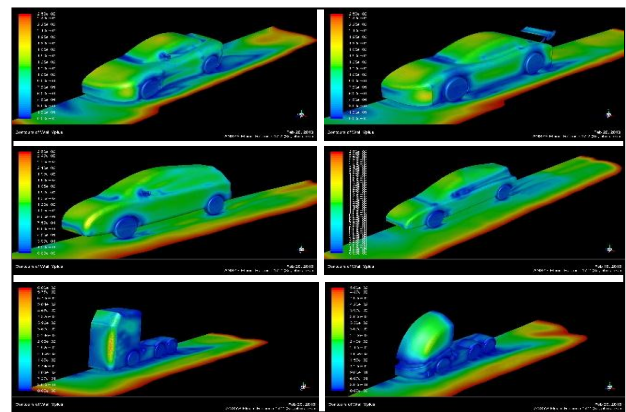


**Fig.12** Contours of Wall  $y^+$

**Table 6** Comparative results of  $C_D$  and  $C_L$  between high and low meshes

Geometry	High Mesh	Low Mesh	High Mesh	Low Mesh
	$C_D$	$C_L$	$C_D$	$C_L$
Ahmed body	0.286	0.381	0.352	0.475
Sedan	0.364	0.303	0.476	0.369
Modified Sedan	0.262	0.488	0.328	0.546
CUV	0.22	-0.173	0.294	-0.113
Modified CUV	0.20	-0.719	0.291	-0.785
Truck	0.533	0.416	0.687	0.511
Modified Truck	0.35	0.184	0.492	0.216

Table 6 shows the comparative drag and lift co-efficient values between high mesh and low mesh geometries. By reducing cell element sizes (Table 1), it was possible to produce a more accurate drag & lift coefficient. Reducing the size of the mesh attached to the car surface and its growth rate has a significant effect on the solution and they are considered the most important parameters, nevertheless  $y^+$  has to be within the valid range [11].

**Table 7** Drag reduction rate comparison

Car Type	Modifications Performed	$C_D$ (before)	$C_D$ (after)	Drop rate %
Sedan	Roof Drop, Wing Mirror, Spoiler, Underbody Hoist	0.364	0.262	28.02 %
CUV	Roof Drop, Diffuser Hoist, Boat Tailing, Underbody Hoist	0.22	0.20	9.09 %
Truck	Roof Drop, Wing Mirror, Underbody Hoist	0.533	0.35	33.96 %

Table 7 shows the modifications performed on each vehicle and the rate of drag reduction after those modifications. The drag reduction rate in the Sedan and Truck type vehicle is significant compared to Crossover Utility Vehicle (CUV).

From Fig.13 it is apparent that the  $C_D$  conditions had been improved in the modified ones.

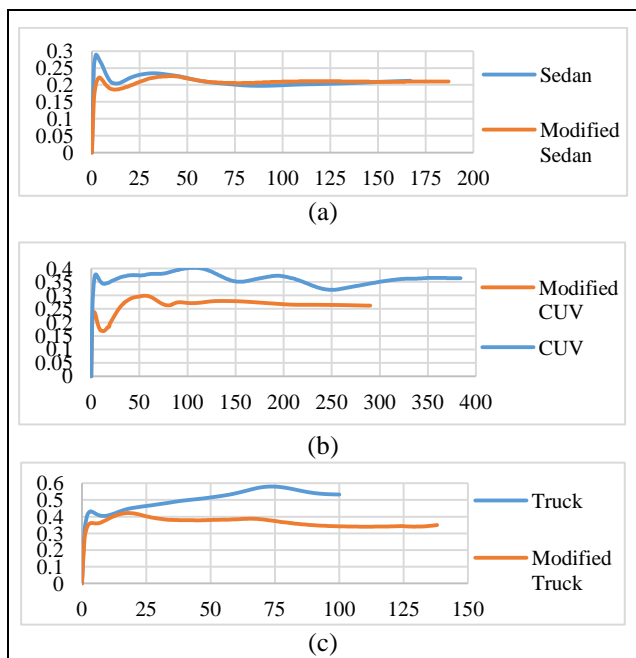


**Fig.13** Comparative  $C_D$ (Y-axis) vs Iteration (X-axis) plots for (a) Sedan & Modified Sedan (b) CUV and Modified CUV (c) Truck and Modified Truck

## 7. Conclusion

Aerodynamic characteristics of several ground vehicles had been analyzed by CFD and the results were found to be in reasonable agreement with the computational value of Ahmed Body. As modifications in the geometries of the original models led to a significant drag reduction rate of 28.02% for Sedan, 9.09% for CUV, and 33.96% for Truck type vehicle, therefore, it can be concluded that the CFD simulations produced satisfactory results. Also, based on the mesh dependency study, it is safe to assume that more accurate results are obtainable if further mesh refinement can be continued. This will eventually lead to positive performance characteristics (lift and drag), therefore, improving the overall performance of the vehicles.

## REFERENCES

- [1] European Commission. 2014b, *Innovation Union Scoreboard*, 2014
- [2] Bettes, WH. "The Aerodynamic Drag of Road Vehicles – Past, Present and Future" *Engineering & Science*, January 1982, 4-10.
- [3] Lundberg, A., Hamlin, P., Shankar, D., Broniewicz, A. et al., "Automated Aerodynamic Vehicle Shape Optimization Using Neural Networks and Evolutionary Optimization", *SAE Int. J. Passeng. Cars - Mech. Syst.* 8(1):242-251, 2015
- [4] "ANSYS FLUENT will", 18.1 Overview of Flow Solvers, 2009, January 23
- [5] Thet Mon Soe, San Yu Khaing, "Comparison of Turbulence Models for Computational Fluid Dynamics Simulation of Wind Flow on Cluster of Buildings in Mandalay", *IJSRP* 7(8) (ISSN: 2250-3153), 2017
- [6] Damjanovic, D., Kozak, D., Živić, M., Ivandic, Z., Baškarić, T., "CFD analysis of concept car in order to improve aerodynamics", *International Scientific and Expert Conference TEAM 2010*, Kecskemét, November 4-5, 2010
- [7] Ahmed, Syed R., G. Ramm, and G. Faltn. "Some salient features of the time-averaged ground vehicle wake." *SAE Transactions: p473-503*, 1984
- [8] Davis, N., "FLUENT Lab Exercise 10 - Ahmed Car Body", *Illinois: Computational Science and Engineering Illinois*, 2015
- [9] Jathar, L.D., Borse, S.L. , "Study of Flow over Car by Changing Different Parameters using Open Foam", *ISSN 0974-3138* Volume 6, Number 1, 2014
- [10] Meile, Walter & Brenn, Günter & Reppenhagen, Aaron & Lechner, Bernhard & Fuchs, Anton. "Experiments and numerical simulations on the aerodynamics of the Ahmed body", *CFD Letters* 3, 2011
- [11] Bayraktar, I., Landman, D., and Baysal, O., "Experimental and Computational Investigation of Ahmed Body for Ground Vehicle Aerodynamics," *SAE Technical Paper* 2001-01-2742, 2001.